Iranian Polymer Journal
15 (8), 2006, 645-653

Availlable online at: http://journal.ippi.ac.ir

Preparation and Characterization of Polystyrene/ Montmorillonite Nanocomposite by Melt Intercalative Compounding

Belkacem Zidelkheir [1*], Soufiane Boudjemaa [1], Mahmoud Abdel-Goad [2], and Brahim Djellouli [3]

(1) Laboratoire de Chimie Organique, Département de Génie des procédés, Université Mohamed Boudalf, 28000, M'sila, Algérie
(2) Institute of Polymer Research Dresden, Hohe Strasse 6, D-01069, Derseden, Germany
(3) Laboratoire de Génie des Procédés Chimiques (LGPC), Université Ferhat Abbas , 19000, Setif, Algérie

Recieved 5 March 2006 ; accepted 15 August 2006

ABSTRACT

Polymer composites based on modified montmorillonite (OMMT) and polystyrene (PS) were prepared with different compositions by melt processing. The pristine montmorillonite (MMT) was obtained from Algerian plant with a cation exchange capacity (CEC) of 119 meq/100 g. The modification of MMT was carried out by treating with octadecylammonium cation. The polymer composites were characterized using different techniques such as X-ray diffraction (XRD), infrared spectrophotometery (IR), differential scanning calorimetery (DSC), thermal gravimetric analysis (TGA), and rheology and tensile measurements. The results were showed that, the basal space of the silicate layer increased, as determined by XRD, from 12.6 to 32.3 Å. The microstructure was detected by X-ray patterns and transmission electronic microscopy (TEM) at 2 wt% OMMT, however, higher than 2 wt% OMMT reveals partial intercalation structure. The composite with 5 wt% was indicated the greatest improvement in thermal stability. The rheological properties of the PS/OMMT composites were investigated using ARES-rheometer operated in the dynamic mode with a parallel plate geometry. The storage and loss moduli were increased with increasing the clay content. The stress-at-break is also improved relatively compared to the virgin polystyrene in our experimental conditions.

Key Words:

montmorillonite;
composite;
melt intercalation;
polystyrene;
rheology;
thermal stability.

(*)To whom correspondence to be addressed.
E-mail: bzidelkheir@yahoo.fr

INTRODUCTION

Nowadays progress in polymer-clay nanocomposites (PCNs) have attracted considerable studies on preparation and characterization of these new class of materials which can exhibit unexpected and unique properties such as mechanical strength, thermal stability, gas barrier properties, chemical and solvent resistance, and other interesting properties [1].

Polymer melt intercalation presents a great advantage in production of PCNs over conventional polymer processing techniques. Compared to other synthesis methods, it is generally the most used, and environmentally friendly (no solvent is required) technique. Applicable to a variety of polymers, from the non-polar polystyrene (PS) to a strongly polar systems as nylon [2], the melt

intercalation method is carried out by melt mixing of a polymer and an organically modified montmorillonite (OMMT). Two morphologies of polymer/clay nanocomposites have been widely studied: intercalated and exfoliated structures.

Intercalated structure is in general obtained when the polymer is located between the silicate layers; even though the layer spacing increases, there are still attractive forces between the silicate layers to stack the layers in uniform manner and thermodynamically stable spacing. Exfoliated structure consists of nanometer-thick silicate layers dispersed in a polymer matrix, which result from extensive penetration of the polymer within the interlayer spacing. Delamination of the crystallites can be observed because there are no longer sufficient attractions between the silicate layers to maintain uniform layer spacing. Recently, various aspects of PCNs have been investigated [3-8].

At first, the organic intercalating agent and its properties (swelling, exchange capacity, density in clay gallery and enlargement involved in the basal spacing, etc.), second, the thermal stability of the organic clay (which is the key factor in the melting process performed usually at high temperature). The effect of mixing conditions, simple annealing without shear, shear mixing, temperature and residence time, constitute other important factors in the optimisation of the fabrication of the well dispersed layered silicates in the polymer matrix [4]. Due to the large surface area of nanoparticles, the strong interparticles interactions make dispersion of the nanofillers particles very difficult. This limitation is overcome by the organic modification of the layered silicates to form the so called organoclay. These are produced by replacing the cation originally present in the galleries with one organic cation such as ammonium, sulphonium and phosphonium cations containing at least one long n-alkyl chain. The aliphatic tail renders organophylic the normally hydrophilic silicate surface [9].

The rheological properties of polymer/clay nanocomposites are determined by a combination of mesoscopic structure and the strength of the interaction between the polymer and clay. The mesoscopic structure depends not only on the strength of polymer/ clay interaction but also on the inherent viscoelastic properties of the matrix in which the clay layers are dispersed. Due to this kind of internal structure, polymer/clay nanocomposites have provided important characteristics of the static and dynamic properties of confined polymer including viscoelastic properties [4, 9-11].

In the present work, Algerian montmorillonite was organophilized and tested to prepare nano-composite by melt blending. The results in terms of thermal, rheological, and mechanical properties of nano-composite were presented as a function of clay contents. These results are really encouraging compared to other clays.

EXPERIMEMTAL

Materials

Polystyrene (PS) was supplied by BASF. The octadecylammine was purchased from Flucka. The sodium montmorillonite was provided by Maghnia plant, Algeria, and used without further purification.

Organophilized Montmorillonite Preparation

This procedure applies to all layered minerals capable of cation-exchange that disperse but do not dissolve in solutions containing water and/or a polar organic solvent such as alcohol or ketone. The following procedure is described for the preparation of primary octadecylammonium-modified montmorillonite (OMMT).

8 g of sodium montmorillonite (119 meq/100 g cation exchange capacity) was dispersed into 500 mL of hot water (80°C) with continuous stirring. 3.1 g of primary octadecylammine and 1.15 mL of concentrated hydrochloric acid (35%) were dissolved into 200 mL of distilled hot water (80°C) with continuous magnetic stirring using a larger Teflon-coated stir bar. The dissolution of the surfactant occurred, typically within an hour. Once a clear solution of surfactant was obtained, it was poured into the well-mixed layered silicate dispersion, at which time octadecylammonium-modified montmorillonite was observed. In order to ensure a complete reaction, the mixture was allowed to continuous stirring at 80°C for at least 3 h. The obtained solution was left to itself at ambient temperature without stirring for approximately 24 h. After that, the precipitate was collected on a filter paper, washed ten times with distilled water at 80°C under the control of $AgNO_3$. The precipitate was dried to obtain a modified montmorillonite with octadecylammonium.

Composites Preparation

Four types of composites of different compositions (2, 4, 5 and 10 wt% OMMT) were prepared by melt compounding at a mixing temperature of 140°C, using an extruder machine with a screw speed of 50 rpm. The residence time was determined when a constant value of the torque was observed. It was maintained at 10 min for all the experiments in order to avoid any material degradation and the reference sample, pure PS, was processed under the same conditions.

Characterization

X- ray diffraction analysis was carried out on a Philips diffractometer (PW-1710) using CuK_α (λ = 1.54 Å) radiation at room temperature. The basal spacing distance of silicate layers were calculated from the estimation of (001) plane peak in XRD patterns using the Bragg's law:

$$d = \lambda /2 \text{ Sin } \theta_{max} \qquad (1)$$

All scanning are performed in 2θ range 2 - 10 degrees. Bright field TEM image of the composites were obtained at 80 kV, with a Zeiss EM 900. The samples were cooled at -80°C and then microtomed with a diamond knife cooled at -60 °C to give section with a nominal thickness of 50 mm and 1 mm^2 of superficial area . The sections were collected on the surface of a solution of dimethylsulphoxide/water, 60/40 parts, respectively, and then transferred on Cu grids of 200 mesh. The DSC analysis was conducted on a Shimadzu DSC-60 calorimeter with N_2 as a purge gas, with a heating rate of 10°C/ min.

The infrared analysis was conducted on a Shimadzu FTIR - 8300 spectrophotometer, using KBr disc method. Thermal gravimetric analysis (TGA) was conducted on a Shimadzu TGA - 51H analyser with N_2 as a purge gas. The melt rheological properties of the material were determined using an ARES-rheometer (Rheometrics Scientific, USA).

In this work the measurements were performed in the dynamic mode and 8 mm parallel plate's geometry with gap settings about 2 mm under nitrogen gas. The strain amplitude was kept in the linear viscoelastic region in the whole frequency range. The measuring temperature was at 200°C as a function of the angular frequency, ω (rad/s). The frequency is varied between 100 and 0.1 radian/s. Tensile strength was estimated through the classic uniaxial tension test on an Instron machine.

To measure the stress-at-break, three specimens were cut and their thicknesses were determined with a Fowler micrometer. Thickness was taken at three different places on the specimen and averaged for stress-at-break calculation. Samples were carefully mounted straight and symmetrically in the grips of the dynamometer tester and then were stressed at a constant strain rate until failure. The stress was calculated using the following definition:

$$S = F/A \qquad (2)$$

Where:

S = stress-at-break
F = applied force
A = cross sectional area

RESULTS AND DISCUSSION

Figure 1 shows the X-ray diffraction patterns of MMT silicate and its corresponding organophilized montmorillonite (OMMT). As shown in this Figure, the peak maximum shifts from 2θ = 6.98° (Figure a), corresponding to basal spacing d_{001} of 12.6 Å, to 2θ = 2.73° (Figure b).That corresponds to an increase in basal spacing from 12.6 Å to 32.3 Å when montmorillonite is organophilized, indicating the incorporation of a considered amount of organic molecules. A second peak at 2θ = 5.69° also appears to correspond to a distance of 15.1 Å. This peak is attributed to the d_{002} of the interlayer distance d_{001} = 32.3 Å. A systematic study (including initial concentration of swelling agent, temperature of cation exchange, and nature of pristine MMT) was carried out to determine the optimal conditions of intercalation and structure of the organic clay. The influences of these different factors constitute a separate study on the stability of the organic modifier in silicate layers under condition of the melt mixing of the polymer and the OMMT.

The FTIR spectra of pristine and its derived organophilized montmorillonite at room temperature, under air condition are illustrated in Figure 2. The absorption bands for MMT are 3625 cm^{-1} (–OH stretching vibration of MMT), 1037 cm^{-1} (Si–O stretching vibrations of MMT), and 524 and 472 cm^{-1}

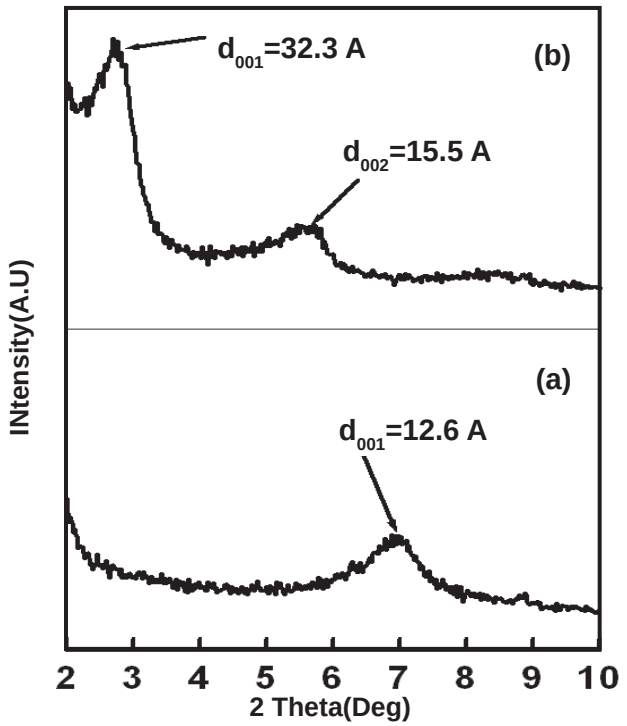

Figure 1. XRD Pattern of (a) MMT- Na and (b) OMMT.

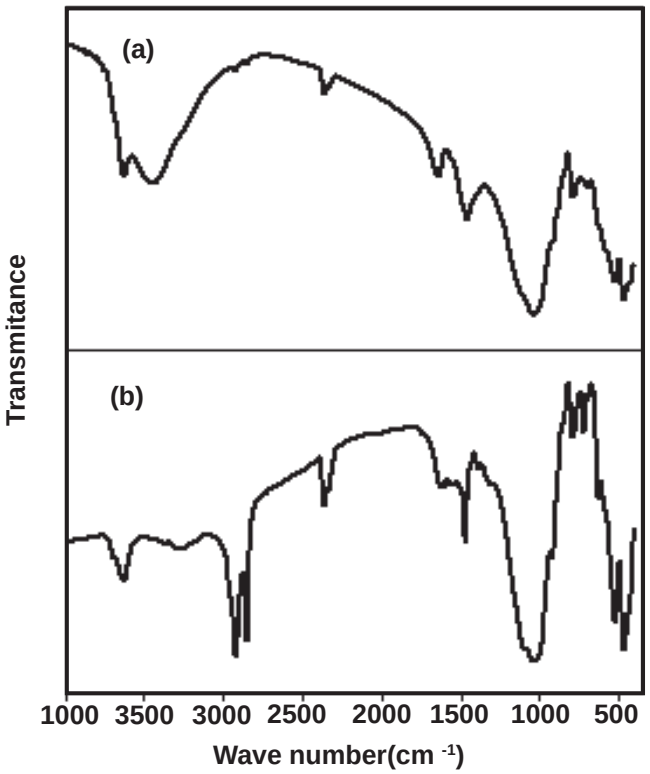

Figure 2. Infrared spectra of (a) MMT-Na and (b) OMMT.

(Al–O stretching and Si–O bending vibrations of MMT, respectively). In the OH stretching region, the band near 3448 cm^{-1} (curve a) is very pronounced in the presence of sodium ion and is related to water content. Also, the C–H asymmetric and symmetric stretching vibration in the alkyl chains of the ammonium salt are 2924 and 2850 cm^{-1}, respectively (curve b). The frequency of asymmetric CH_2 stretching is sensitive to the gauche/trans conformer ratio and the packing density of the chains. The band shift from lower frequencies, characteristics of highly ordered all-trans conformation, to higher frequencies as the number of gauche conformation along the chain increases [6]. The methylene in the all-trans ordered state of crystalline octadecylammine, which is similar to the alkyl chains intercalated into MMT, shows a band at 2920 cm^{-1}. In the intercalated structure, the band shifts to 2924 cm^{-1}, may be due to the increase of the available space in the interlayer space.

The structure and properties of layered silicate composites are usually studied by X-ray diffraction (XRD), transmission electron microscopy (TEM) and dynamic mechanical analysis (DMTA) techniques. Based on the disappearance or the decrease of intensity of XRD peaks, authors conclude the silicate is partially or completely exfoliated [12]. Figure 3 illustrates the XRD patterns of PS/OMMT with different concentration of clay content. As shown in the Figure 3 b, the peak related to clay is disappeared, suggesting that the MMT silicate sheets are exfoliated in PS/OMMT composites. This assumption is greatly supported by the larger gallery distance of the organophilized filler obtained during the cationic exchange process.

A further evaluation of the composite structure by bright-field TEM (Figure 4) indicates micro-sized structure where can be seen the primary particles composed of many silicate layers. This situation corresponds to that of conventional filled polymer where, at least, the primary particles of few microns are dispersed in the polymer matrix. However, a very small peak is observed at $2\theta = 2.45°$ in the case of PS/OMMT composites containing 4, 5, and 10 wt% OMMT compositions. This small peak can be assigned to some intercalated MMT silicate sheets having basal distances below the critical one.

In the corresponding TEM micrograph (Figure 5) is visible a tactoids, indicating a co-existence of micro-sized and intercalated structures. Figure 6 reveals higher stability of PS/OMMT composites than pure

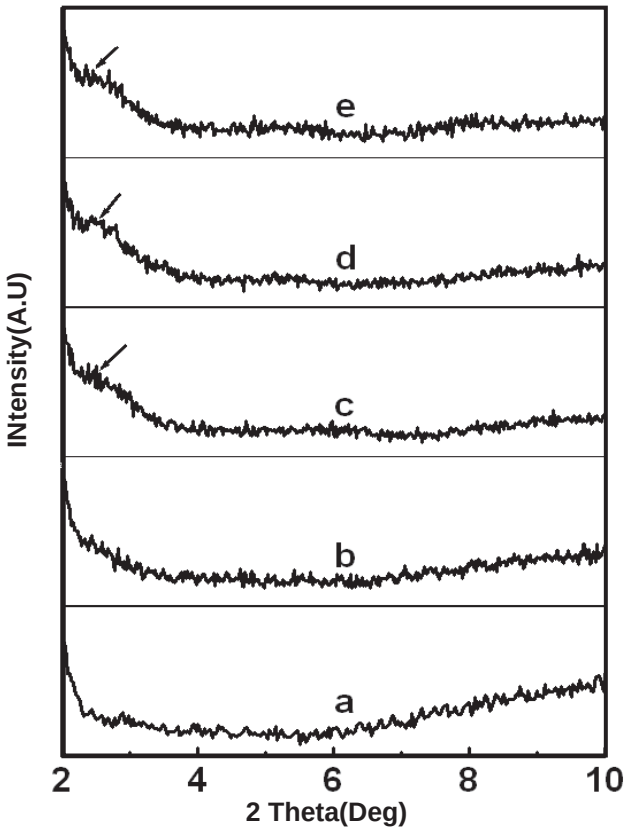

Figure 3. XRD Patterns of PS/OMMT composites with different OMMT contents (melt mixing at 140° C under air condition, 10 min., 50 rpm). (a) 0, (b) 2, (c) 4, (d) 5 and (e) 10 wt% .

PS. Since the onset of decomposition for PS/OMMT composites is shifted toward a higher temperature with the clay content. For instance, at 10% of degradation, the thermal decomposition temperature $T_{0.1}$ was

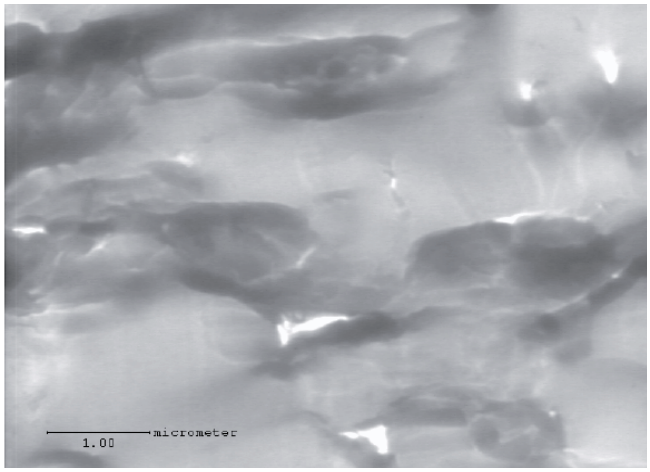

Figure 4. TEM Micrograph of a PS/OMMT micro-sized composite. OMMT loading: 2 wt%.

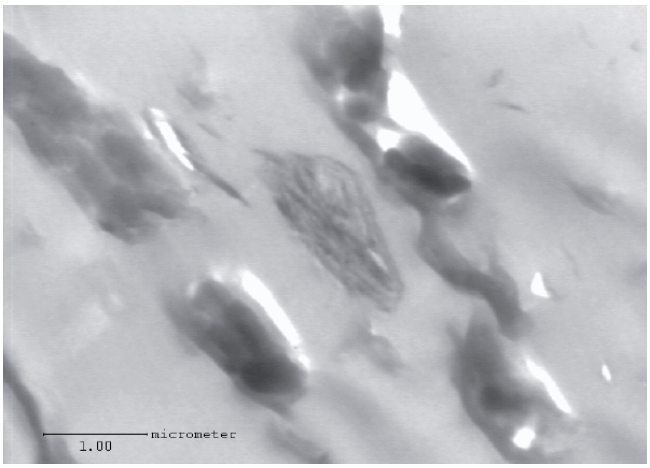

Figure 5. TEM Micrograph of a partial intercalated PS/OMMT composite. OMMT loading: 5 wt%.

increased from 390°C for the neat PS to 394°C for the composites containing 2 , 4, and 10 wt% OMMT (Table 1). However, the composite containing 5 wt% of OMMT shows the highest degradation temperature (406°C). This behaviour is largely maintained throughout the organic decomposition (as shown by the comparable improvement in $T_{0.5,}$ the temperature at which 50% degradation occurs) (Figure 7) [13]. Thus, MMT possesses high thermal stability and its layer structure exhibits great barrier effect to stop the evaporation of the small molecules generated in the thermal decomposition process and effectively limits the continuous decomposition of the PS [14,15].

Similar observation is deduced from the first TGA derivative of PS composites illustrated in Figure 8, where the peak indicates the temperature at a maximum

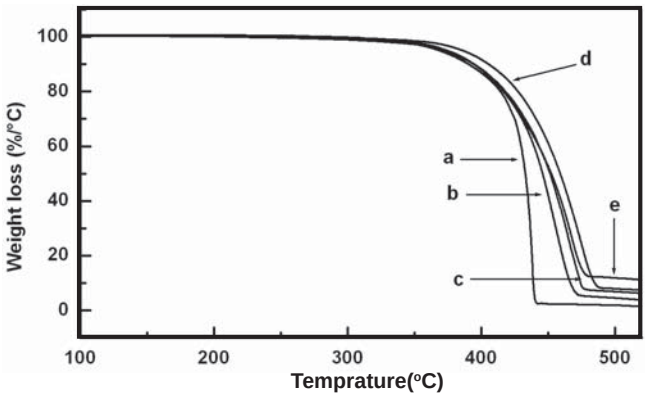

Figure 6. TGA Thermograms of weight loss versus temperature under N_2 flow of PS / OMMT composites (melt mixing at 140°C under air condition, 10 min., 50 rpm): (a) 0, (b) 2, (c) 4, (d) 5 and (e) 10 wt% .

rate of degradation, delayed at a higher temperature (Table 1). The insertion of PS inside the interlayers can be ascribed to both the ion-induced dipole force between clay layers and PS, and the contraction of the gallery height due to water removal. Dietsche and Mulhaupt [16] also observed an improved thermal stability of acrylic composites using TGA technique. The relatively strong fixation between polymer and inorganic surface is also considered to be due to the cooperative formation of ion induced dipole forces [17].

In addition, Chen at al. [18] suggested that the higher decomposition onset temperature of a PS/OMMT composite as compared to that of PS, can be attributed to the nanoscale MMT layers, preventing out-diffusion of the volatile decomposition products. This may be the reason why the PS/OMMT composite exhibited higher thermal stability than virgin PS.

To investigate the mobility of PS chains in term of its T_g (glace transition temperature) in the clay layers , DSC study of pure PS and PS/OMMT hybrids has been carried out (Figure 9). The glass transition temperature was determined at the inflection point between the onset and the end set temperatures. The T_g of the composites was remarkably increased relatively to the neat polystyrene, but slightly as the OMMT content increases. This is clearly caused by the strong interaction between OMMT and PS, which limits the cooperative motions of the PS main chain segments [19]. The different values are summarized in Table 1.

Table1. Degradation and glass transition temperatures of PS/OMMT composites with various OMMT contents (wt%) prepared at a processing temperature equals to 140°C: (a) 0 ; (b) 2 ; (c) 4 ; (d) 5 ; and (e) 10 wt%.

Thermal properties	a	b	c	d	e
temperatuure at 10% degradation(°c)	390	394	394	406	394
temperatuure at 10% degradation(°c)	432	446	451	459	452
temperatuure at maximum rate of degradation (°c) measured by (TGA)	437	455	466	476	468
Glass transition temperatuure at (°c) measured by (DSC)	89.8	93.1	93.1	93.5	93.8

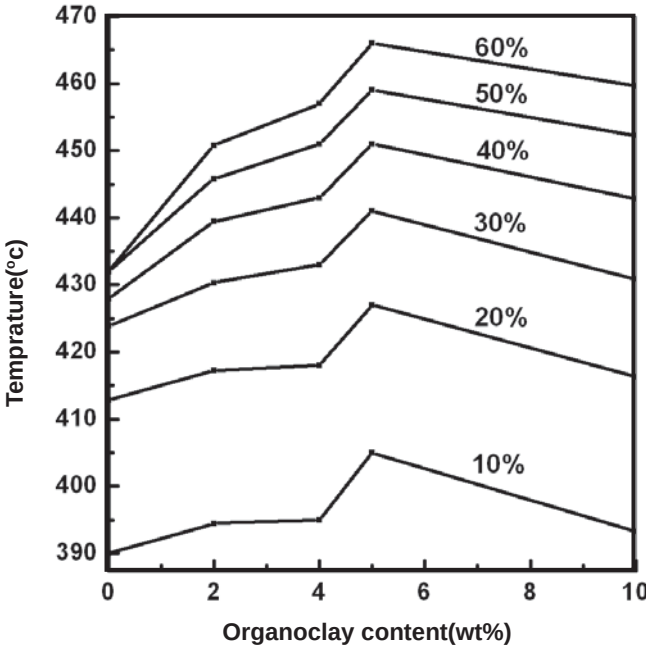

Figure 7. Decomposition temperature of OMMT composites , (melt mixing at 140°C under air condition, 10 min, 50 rpm).

Linear viscoelastic responses, such as storage modulus (G′) and loss modulus (G″), of unfilled (neat) and filled PS are logarithmically plotted at 200°C as a function of angular frequency in Figures 10 and 11, respectively. As the silicate loading increased, both

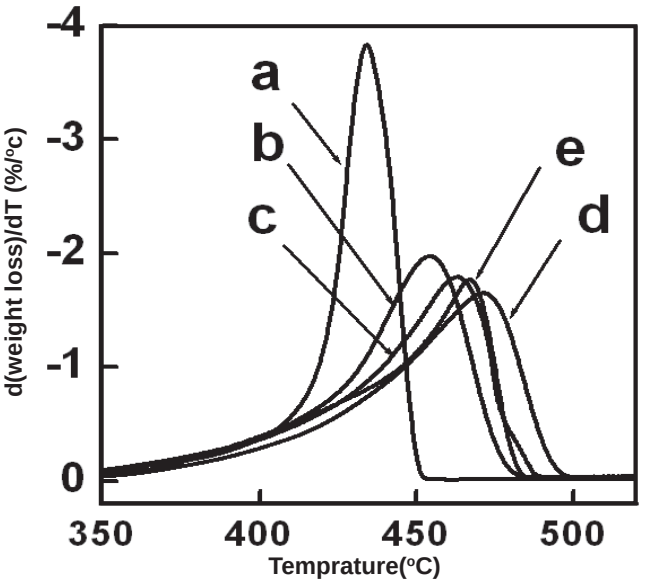

Figure 8. TGA Derivative of PS/OMMT composites with different OMMT contents, (melt mixing at 140°C under air condition, 10 min., 50 rpm): (a) 0 ; (b) 2; (c) 4; (d) 5 and (e) 10 wt% **.**

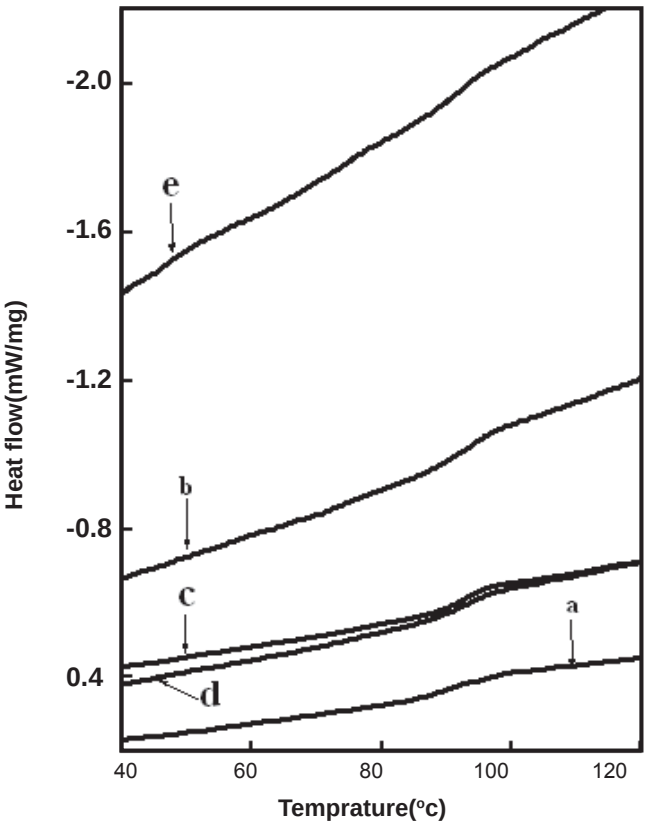

Figure 9. DSC Thermograms of PS/OMMT composites with various OMMT content, (melt mixing at 140° C under air condition, 10 min., 50 rpm): (a) 0; (b) 2; (c) 4; (d) 5 and (e) 10 wt%.

G′ and G″ show monotonic increase along the entire frequency range. These Figures show that the dynamic mechanical moduli of the PS composites are higher than

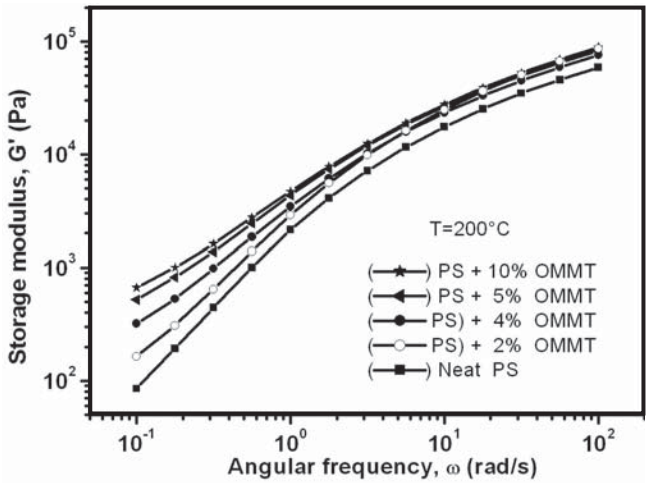

Figure 10. G′ of PS composites as a function of angular frequency at T = 200°C.

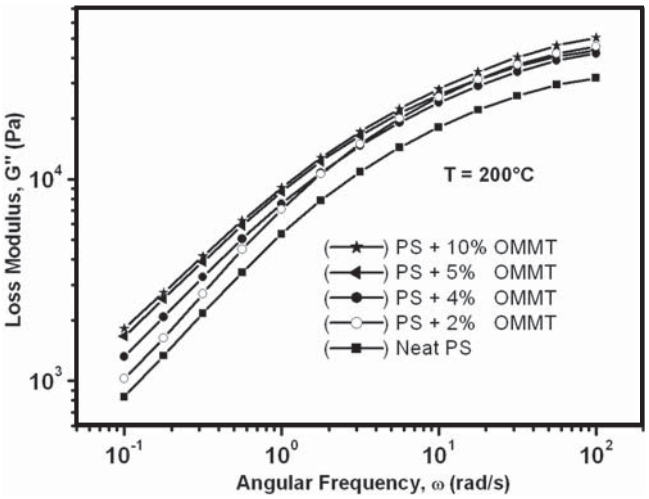

Figure 11. G″ of PS composites as a function of angular frequency at T = 200°C.

those of neat PS, in particular at low frequencies, the difference is significant. However, the difference in the dynamic moduli values between PS+10 wt% OMMT and PS+5 wt% OMMT is minimum. The G′ has slopes of 0.95 (PS), 0.89 (PS+2 wt% OMMT), 0.78 (PS+4 wt% OMMT), 0.75 (PS+5 wt% OMMT), and 0.70 (PS+10 wt% OMMT) while G″ has slopes of 0.52 (PS), 0.55 (PS+2 wt % OMMT), 0.49 (PS+4wt% OMMT), 0.46 (PS+5 wt% OMMT), and 0.47 (PS+10 wt% OMMT) in log plots indicating that at the lowest frequencies, the response of the system exhibits liquid-like behaviour (G″> G′). However, the two moduli soon become equal and display nearly a plateau region, having higher G′ than G″.

In this region, PS/OMMT nanocomposites show glassy solid-like behaviour [20]. This characteristic transition (from liquid-like to solid like behaviour) shifts to the low frequency region as the OMMT loading increases. Similar trends in the oscillatory shear experiment were also observed by Krishnamoorti and Giannellis [21] for a series of nylon6/MMT and poly(e-caprolactone)/MMT composites for the polymer chains being end tethered to the silicate surface via a cationic surfactant. The slope and absolute values of the dynamic moduli indicate a super molecular structure formation in the composite [22]. The higher was the G′ and the smaller was the slope, the more pronounced was the interaction between the silicate sheets and their tendency to form a 3-dimentional superstructure [23].

Rheological measurements performed on PS-based model composites have shown that the formation

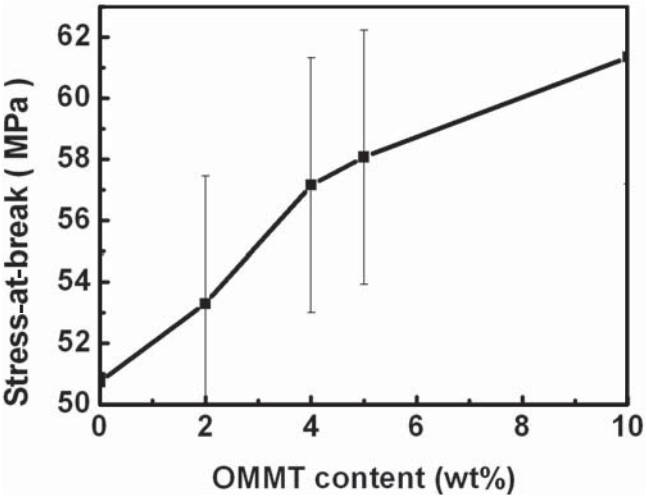

Figure 12. Stress-at-break of PS/OMMT composites versus OMMT content (wt %).

of a superstructure results in a well-pronounced equilibrium plateau modulus [24]. In thermoplastic-based (intercalated or exfoliated) composites, the stress-at-break, which expresses the ultimate strength, may vary strongly depending on the nature of the interactions between the matrix and the filler [1]. The stress-at-break of PS/OMMT composites versus organophylic montmorillonite content curve is displayed in Figure 12.

As expected, the silicate reinforced systems show a superior strength relatively to ordinary polystyrene. It is obvious that even with the addition of such a low loading of montmorillonite (2-10 wt%), the stress-at-break increases considerably. For instance, compared to unfilled polystyrene, the 5 wt% clay composite has around 15% higher tensile strength. However, the 10 wt% clay composite has only 21% higher tensile strength than that of unfilled polystyrene. In other hand, the increase of the stress-at-break is more pronounced between 0 and 5 wt% OMMT content. This observation can be attributed to the strong interaction between PS and OMMT, but it appears to increase slightly above 5 wt% filler loading, may be due to inevitable aggregation of the silicate layers in high clay content.

CONCLUSION

Different PS/OMMT composites were prepared via melt intercalation process using an extruder machine. Algerian montmorillonite was ionically exchanged by octadecylammonium cation. The polymer composites were characterized using different techniques such as X-ray diffraction (XRD), transmission electronic microscopy (TEM), infrared spectroscopy (IR), differential scanning calorimetery (DSC), thermal gravimetric analysis (TGA), and rheology and tensile measurements.

The results showed that, the basal space of the silicate layer increased. From the XRD spectra and TEM micrographs, micro-sized structure of PS/OMMT composite was detected at 2 wt% OMMT loading, however, at a higher OMMT content, a partial intercalated structure was formed. The composite with 5 wt% indicated the greatest improvement in thermal stability. The rheological and mechanical properties were improved by the incorporation of clay into PS. Since the stress-at-break was improved relatively to the virgin polystyrene. The G′ and G″ values of PS/OMMT composites showed also a monotonic increase with OMMT loading.

ACKNOWLEDGEMENT

This work was supported financially by the University of M'sila and by the Algerian Ministry for University and Research (MESRS, Project Number J1901/01/02/2003). Both are gratefully acknowledged.

REFERENCES

1. Alexandre M., Dubois P., Polymer layered silicate nanocomposites:Preparation, properties and new class of materials, *Mater. Sci. Eng. R.*, **28**, 1-63, 2000.
2. Giannelis E. P., Polymer layered silicate nanocomposites, *Adv. Mater*., **8**, 29-35, 1996.
3. Vaia R. A., Jandt K. D., Krammer E. J., Giannelis E. P., Microstructural of melt intercalated polymer-organically modified layered silicates nanocomposites,*Chem.Mater.*,**8**, 2628-2635, 1996.
4. Giannelis E. P., Krishnamoorti R., Manias E., Polymer-silica nanocomposites: Model systems for confined polymers and polymer brushes, *Adv. Polym. Sci.*, **118**, 108-147, 1999.
5. Lee J. W., Lim Y. T., Park O. O., Thermal characteristics of organoclay and their effects

upon the formation of polypropylene/organoclay nanocomposites, *Polym. Bull.*, **45**, 191-198, 2000.
6. Yoon J. T., Jo W. H., Lee M. S., Ko M. B., Effects of comonomers and shear on the melt intercalation of synthetics/clay nanocomposites, *Polymer*, **42**, 329-336, 2001.
7. Xie W., Hwu J. M., Jiang G. J., Buthelezi T. M., Pan W. P., A study of the effect of surfactants on the properties of polystyrene-montmorillonite nanocomposites, *Polym. Eng. Sci.*, **43**, 214- 222, 2003.
8. Beyer F. L., Tan N. B., Dascupta A., Galvin M. E., Polymer layered silicate nanocomposites from model surfactants, *Chem. Mater.*, **14**, 2983-2988, 2002.
9. Shi H., Lan T., Pinnavaia T. J., Intercalated effects on the reinforcement properties of polymer-organoclay nanocomposites, *Chem. Mater.*, **8**, 1584-1587, 1996.
10. Hyun Y. H., Lim S. T., Choi H. J., Jhon M. S., Rheology of poly(ethylene oxide)/organoclay nanocomposites, *Macromolecules*, **34**, 8084-8093, 2001.
11. Choi H. J., Kim S. G., Hyun Y. H., Jhon M. S., Preparation and rheological characteristics of solvent-cast poly(ethylene oxide)-montmorillonite nanocomposites, *Macromol. Rapid. Commun.*, **22**, 320-325, 2001.
12. Liu X., Wu Q., PP/clay nanocomposites prepared by grafting melt intercalation, *Polymer*, **42**, 10013-10019, 2001.
13. Zidelkheir B., Boudjemaa S., Djellouli.B., Melt intercalation , synthesis and characterization of polystyrene montmorillonite nanocomposite, Proc, 40th International Symposium on Macromolecules, Macro 2004, World Polymer Congress, Paris, 4-9, 2004.
14. Burnside S. D., Giannelis E. P., Synthesis and properties of new poly(dimethylsiloxane) nanocomposites,*Chem.Mater.*,**7**, 1597-1600, 1995.
15. Yano K., Usuki A., Kurauchi T., Kamigaito O., Synthesis and properties of polyamide-clay hybrid, *J. Polym. Sci. Pol. Chem.*, **31**, 2493-2498, 1993.
16. Dietsche F., Mülhaupt R., Thermal properties and flammability of acrylic nanocomposites based upon organophylic layered silicates, *Polym. Bull.*, **43**, 395-402, 1999.
17. Chen G., Liu S., Chen S., Qi Z., FTIR Spectra, thermal properties and dispersibility of a polystyrene/ montmorillonite nanocomposites, *Macromol. Chem. Phys.*, **202**, 1189 -1193, 2001.
18. Chen G., Liu S., Zhang S., Qi Z., Self-assembly in a polystyrene/montmorillonite nanocomposite, *Macromol. Rapid. Commun.* **21**, 746 - 749, 2000.
19. Huang J. C., Zhu Z., Yin J., Qian X., Sun Y. Y., Poly(etherimide)/montmorillonite nanocomposites prepared by melt intercalation: Morphology, solvent resistance properties and thermal properties, *Polymer*, **42**, 873 - 877, 2001.
20. Gupta R.K., *Polymer and Composite Rheology*, Marcel Dekker, New York, 2000.
21. Krishnamoorti R., Giannelis E. P., Rheology of end-tethered polymer layered silicate nanocomposites, *Macromolecules*, **30**, 4097- 4102, 1997.
22. Tae H. K., Sung T. L., Lee C. H., Choi H. J., Jhon M. S., Preparation and rheological characterization of intercalated polystyrene/organophylic montmorillonite nanocomposites, *J. Appl. Polym. Sci.*, **87**, 2106-2112, 2003.
23. Hoffmann B., Kressler J., Stoppelmann G., Friedrich C. H., Kim G. M., Rheology of nanocomposites based on layered silicates and polyamide-12, *Colloid. Polym. Sci.*, **278**, 629-636, 2000.
24. Hoffmann B., Dietrich C., Thomann R., Friedrich C., Morphology and rheology of polystyrene nanocomposites based upon organoclay, *Macromol. Rapid. Commun.*, **21** , 57-61 , 2000.